



ORIGINAL RESEARCH ARTICLE

Mineralogical and Structural Analyses of Natural Fluorite from Yantuwaru Mining Site, Nigeria

Gidado Shehu^{*1}  and Ibrahim Muhammad Bagudo² ^{1,2} Department of Physics, Umaru Musa Yar'adua University, Katsina, Nigeria.**ABSTRACT**

Experimental studies of natural fluorite have been reported. In this study, combined X-Ray Fluorescence, FTIR and UV-Vis analyses were performed to give mineralogical information about natural fluorite. The X-ray diffraction technique was also used to determine the crystallographic parameters and structure of the mineral. Results show a variation of Ca contents and low concentration of F, through all fluorite samples due to Ba and Br contents in the samples, causing replacements of impurity ions in the fluorite lattice. REEs in the fluorite samples were to be found responsible for colour. UV-Visible absorption results showed peaks between 209 to 368 nm, which did not affect the fluorite colour. The 224 nm and 365 nm peaks were caused by the electrons and holes trapped in the Ca²⁺ interstitial and vacancy, respectively. The absorption bands in the visible range relate to the corresponding fluorite samples. The FTIR results showed absorptions causing CO₂ and CO₃²⁻ stretching vibration due to the CaCO₃ and OH stretching vibration due to water in the samples. The structural configuration, the lattice parameters and the planes confirmed a cubic structure. Obtained results confirmed them to be Calcium Fluorite, as expected.

ARTICLE HISTORY

Received February 12, 2023

Accepted March 24, 2023

Published March 30, 2023

KEYWORDS

XRF, XRD, FTIR, UV-VISIBLE, REEs, Fluorite.

© The authors. This is an Open Access article distributed under the terms of the Creative Commons Attribution 4.0 License (<https://creativecommons.org/licenses/by-nc/4.0/>)

INTRODUCTION

Fluorite or calcium fluoride (CaF₂) is a naturally occurring mineral popularly known as fluorspar. The mineral is remarkable, with a variety of brilliant, attractive colours ranging most commonly from light to dark blue. Apart from the blue colour appearance in fluorite, the appearance of red, purple, yellow, green, and white also occur. It is however colourless when in its purest form (Balogun *et al.*, 1996; Akhter *et al.*, 2018). It has fluorescence under cathode-ray and ultraviolet irradiation (Ge *et al.*, 2022).

Fluorspar of various origins has consistently been reported to have these extremely different colours due to physical disturbance in the crystalline structure and the compositional variation due to impurities as inclusions and traces of other elements. For example, green fluorite usually contains Sm²⁺, Dy³⁺, and Tm²⁺. Yellow fluorite is often due to Yb³⁺, while, Gd³⁺ presence is the reason why fluorite is red (Ge *et al.*, 2022). The optical property of fluorescence in fluorite may also be due to the impurities present in the mineral. These impurities significantly modify other properties such as the electrical and thermal luminescence of minerals (Balogun *et al.*, 1999; Mao *et al.*, 2015; Altay, 2020).

Fluorite may contain radioactive elements such as Th and U which usually irradiate it to form colloidal calcium and an F⁻ centre (Ge *et al.*, 2022).

Fluorite has a cubic face-centered lattice which is divided into eight parts. A fluorine ion is surrounded by four Ca ions at the centre of each smaller cube. Each Ca is coordinated by eight F ions arranged at the corners of a regular tetrahedron (Akhter *et al.*, 2018). However, in the crystal structure of fluorite, Ca sites are often occupied by transition metal elements such as Cr, Mn, Fe and Zn or alkaline elements like Na, K, or rare-earth elements (REEs). In addition to its attractive appearance and beautiful luminous colour, fluorite is also rich in mineral resources (Ge *et al.*, 2022). Based on this, it is significant to explore the value of natural fluorite.

Fluorspar is used in ceramics and as a raw material for the manufacture of toothpaste. It is also used for optical purposes when it occurs in colourless form and to manufacture some chemicals such as hydrofluoric acid and aluminium fluoride. In metallurgical processes, Calcium Fluorite is used as a flux to reduce

Correspondence: Shehu, G. Department of Physics, Umaru Musa Yar'adua University, Katsina, Nigeria.

✉ sgidado1305@gmail.com; 08039634788

How to cite: Gidado Shehu and Ibrahim Muhammad Bagudo. (2023). Mineralogical And Structural Analyses of Natural Fluorite from Yantuwaru Mining Site, Nigeria. *UMYU Scientifica*, 2 (1), 53 – 61. <https://doi.org/10.56919/usci.2123.007>

the temperature of a metallic ore (Akhter *et al.*, 2018). In high background radiation areas such as those surrounding nuclear installations, it is found to be an excellent candidate for environmental radiation dosimetry due to its high luminescence sensitivity to gamma and other ionising radiations (Balogun *et al.*, 1996; Dantas *et al.*, 1998; Polymeris, 2006).

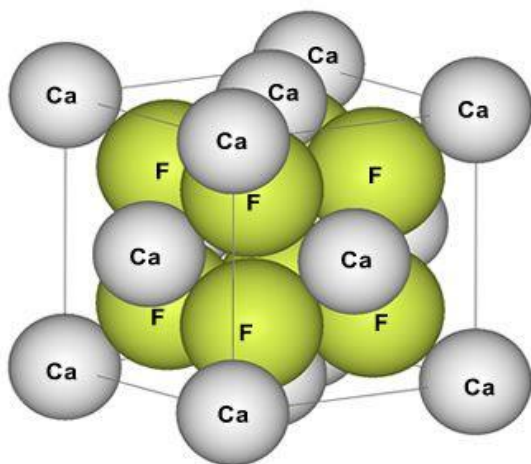


Figure 1: Structure of fluorite (Source: <http://commons.m.wikimedia.org/wiki/File:Fluorite-unit-cell-3D.png>)

Various ore deposits including fluorite deposits are formed by metamorphic rocks intruded by numerous alkaline granitoid. Fluorite deposits, in particular, are formed mostly due to hydrothermal processes (Dill *et al.*, 2016; Öztürk *et al.*, 2019).

In Nigeria, it occurs in the Middle Benue Valley and some other northern parts of the country (Balogun *et al.*, 1996). Elemental trace of constituents of a given mineral deposit as a function of its geological history determines the physical properties of the mineral. It modifies the use to which it could be put. It also helps determine the level of harmful substances that may be found in a given material. The elemental composition of natural fluorite varies based on the deposits' geological origins or placements (Balogun *et al.*, 1996; Polymeris *et al.*, 2006).

The procedure of structure determination aims to obtain the atomic positions in the unit cell and the lattice parameters from a diffraction experiment. X-Ray diffraction (XRD) can calibrate the well logs in terms of mineralogy and has always been used to determine the unit cell lattice parameters and crystal structure of a material by referencing the relative peak intensities (Jozanikohan *et al.*, 2016). The importance of Bragg's Law in quantitative phase analysis cannot be overemphasized (Smaalen, 2013).

X-ray diffraction technology is based on crystal constructive interference of monochromatic X-rays and a crystalline sample. This is fundamental in the research of multi-phase mixtures to determine relative amounts of mineral phases (Kaduk *et al.*, 2021; Balaram *et al.*, 2022). The identification of all crystalline mineral phases is achieved by comparing the measured diffraction data to a reference database (König, 2021).

A large amount of data for such minerals has been systematized by applying geometry and group theory. This data has always been obtained from the Inorganic Crystal Structure Database (ICSD). ICSD is the world's largest free database for identified inorganic crystal structures (Fawcett *et al.*, 2017). The ICSD database provides insight into a material's structural and crystallographic properties, allowing for phase identification using powder diffraction techniques (Jenkins *et al.*, 1987; Gates *et al.*, 2019).

To the best of our knowledge, there has not been any research on the fluorite mineral existing in Yantuwuru local mining site located in Faskari local government of Katsina State. This study is therefore designed to fill this gap.

MATERIALS AND METHODS

Sampling procedure

Yantuwuru mining site (Figure 2.1 (a) and (b)) is located within Ruwan-Godiya Ward, Faskari Local Government Area of Katsina. It is found between 11°45'33"N and 7°12'53.8"E (<http://nigeria.places-in-the-world.com/9411136-region2-ruwan-godiya.html>).

The natural fluorite samples used in this study were collected from ten (10) locations in the Yantuwuru mining site in Katsina State of Nigeria. These samples were transported in fine polyethylene sample containers to Umaru Musa Yar'adua University for analysis. Fluorite A and H were bluish-green in colour. Fluorites B and C were green. However, Fluorites D, E, F and G were all black, except for Fluorite E, which was partially red on one edge. Fluorites I and J had a light-purple appearance on their edges, in addition to the light-green and dark-green colours, respectively in them (Figure 3). The samples were washed separately at the University's central laboratory with water to remove surface contaminants, ground in to powder form and labelled. A portion of each of the ground samples was used for analysis.

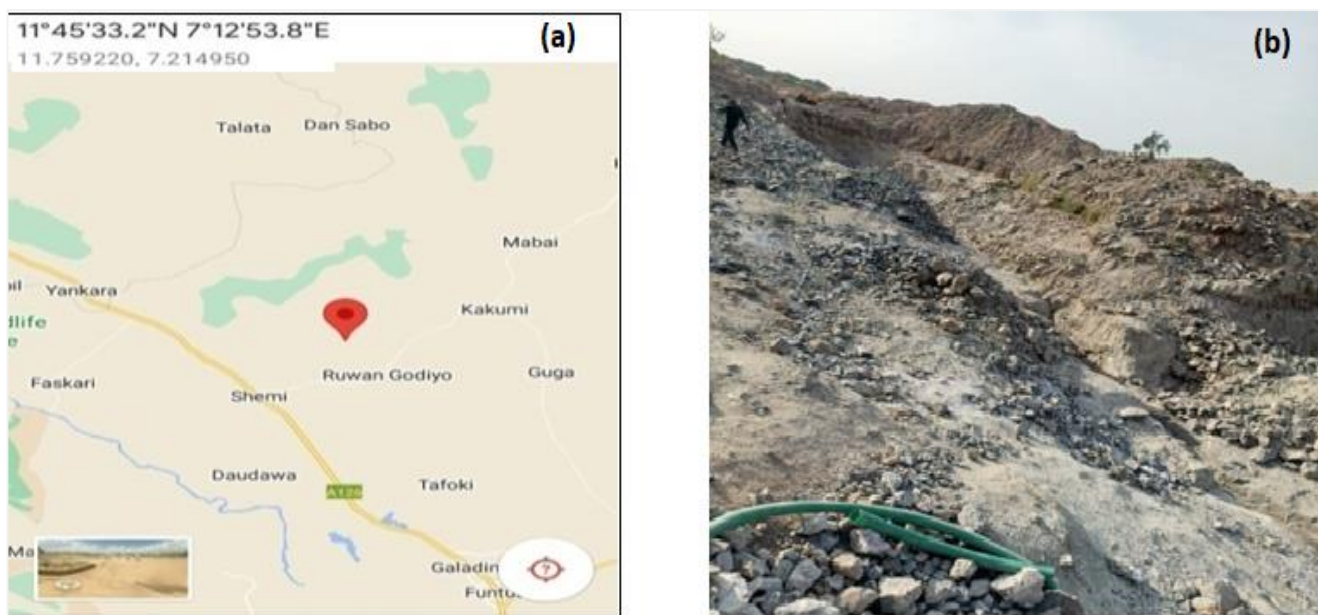


Figure 2: (a) and (b) GPS point and picture of the study area

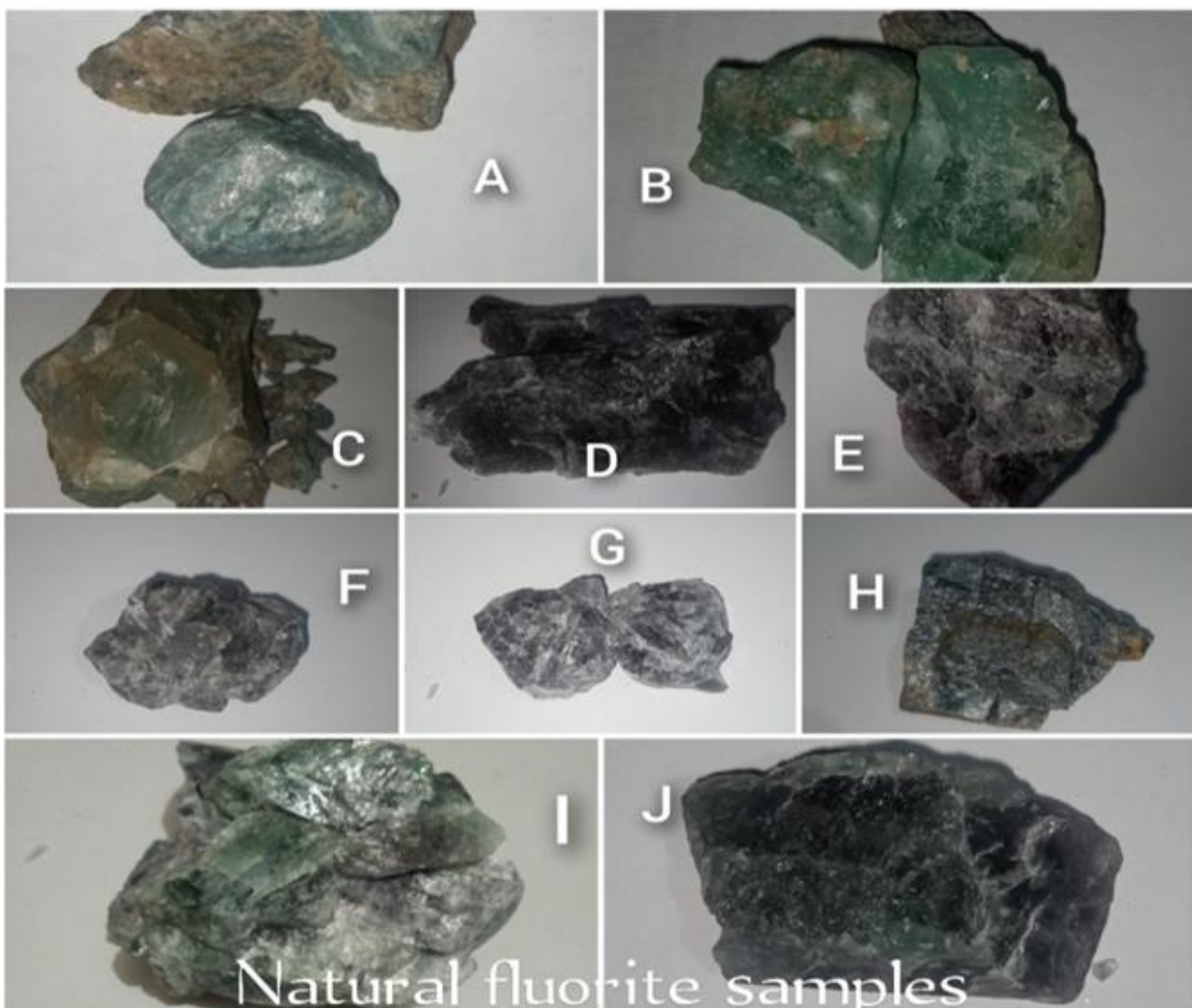


Figure 3: Different samples of natural fluorite

Instrumentation

Energy Dispersed X-ray Fluorescence (EDXRF) technique using *ARL.QUANT'X Analyzer* model was used. EDXRF experiment was run with all the fluorite samples to investigate variations in trace and minor impurities compositions that might influence their physical properties.

The powder X-ray diffraction (XRD) analyser was the Philips X'Pert Diffractometer4kW powder diffractometer. Under the experimental conditions consisting of copper target K α Radiation source ($\lambda = 1.5406\text{\AA}$) and tube voltage and current of 40 kV and 80 mA, respectively.

A UV-6300PC Double Beam Spectrophotometer model was used. The reflection method was used as the experimental test method within the 200–900 nm scan range. The scan step was 5.0nm with a filter precision of 5.

The Fourier infrared spectrometer by Agilent Technologies was used for the infrared spectra test. The transmission method was adopted under the following experimental test conditions: test voltage was 220 V, the resolution was 16cm^{-1} , and the scanning range was $4000\text{--}650\text{ cm}^{-1}$.

RESULTS AND DISCUSSION

X-ray Fluorescence (XRF) Results

The Energy Dispersed X-ray Fluorescence (EDXRF) technique was used to determine the type and quantity in percentage of impurities in the natural fluorite.

Table 1: Average Percentage Concentrations of Major and Trace Elements

S/N	Elements	Average Concentration (ppm)	Average Content Variation (ppm)
1	Ca	3581500	343650
2	F	13990	19300
3	Br	57760	82470
4	Ba	3150	8720
5	Sr	1320	6500
6	Cu	2820	8410
7	Fe	2100	4385
8	K	3000	9660
9	Ge	1560	7900
10	Al	59660	83150
11	Ce	41800	56925
12	Th	3336	7600

The XRF results show that the Ca contents from 10 analyses of different fluorites range between 272000 ppm and 616000 ppm. The F content of the samples ranges from 1550 ppm to 20850 ppm. The calculated XRF average Ca content of analyzed fluorite samples is 358150 ppm. This shows that the fluorite samples were mainly composed of Ca. Trace elements in the samples included some transition metal elements (such as Cu, Fe), alkaline earth elements (e.g Sr), and REEs (like Ce, La and Y).

The variation of Ca contents through all fluorite samples is 257500 ppm because the average Ba content is above the detection limit of 100 ppm (Table 1). The low concentration of F may be due to the higher concentration of its substitute Br in the samples with a calculated average content of 58440 ppm. These deviations are caused by the replacement of impurity ions in the fluorite lattice F^- and Ca^{2+} , such as $\text{REE}^{3+} + \text{F}^- - \text{Ca}^{2+}$ or $4\text{Ca}^{2+} - 2\text{REE}^{3+} + \text{Mg}^{2+}$ and so on.

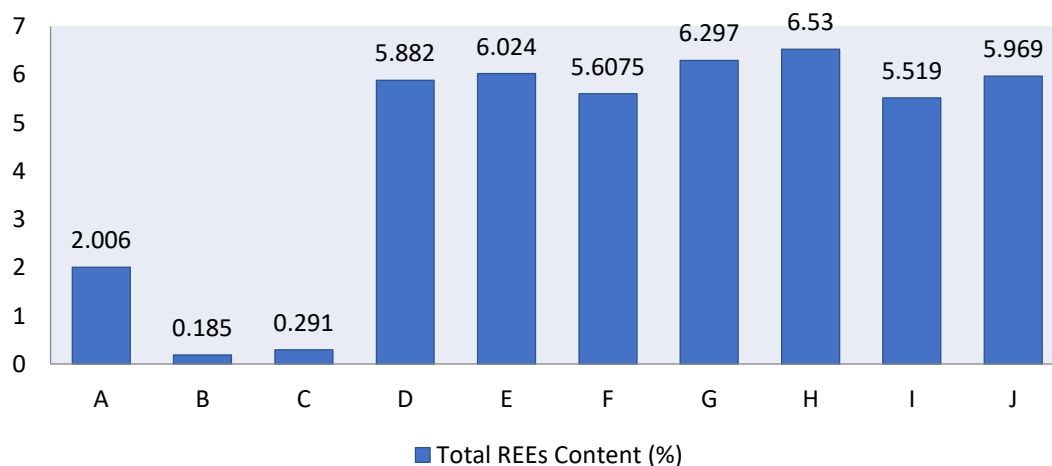


Figure 4: Total content of REEs in each fluorite sample

The concentration of rare-earth ions is responsible for the colour and luminescence of fluorites. Sample B (0.185%) has the least REEs content, followed by sample C (0.291 %). This may be due to their translucent appearance. However, sample A has relatively lower

REEs content, owing to its more translucence, than the other samples D, E, F, G, H, I and J, with relatively close values of REEs concentrations.

X-ray Diffraction Result

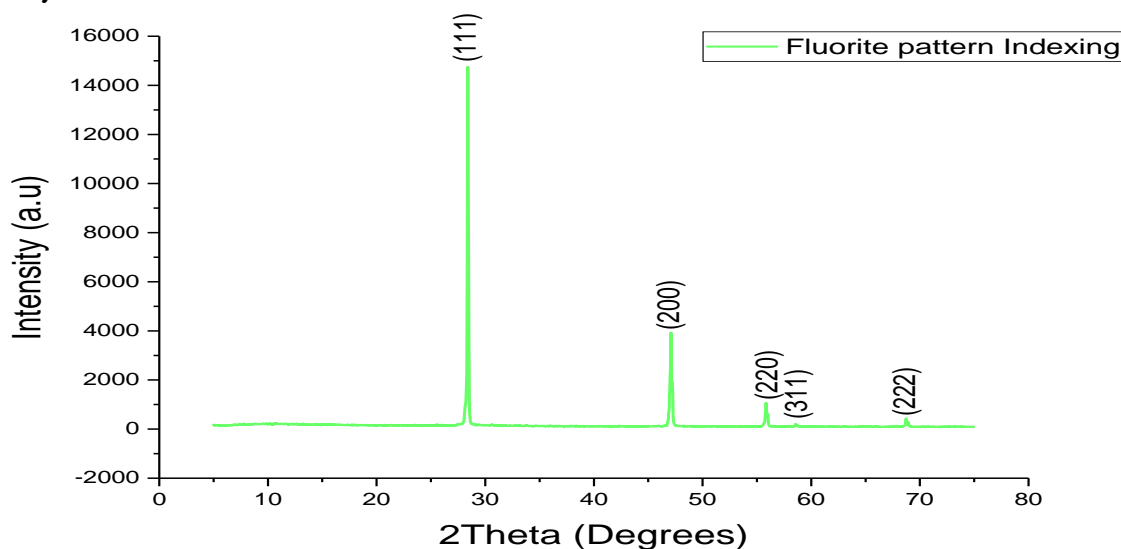


Figure 5: Indexing the XRD patterns for the most matching fluorite

The figure shows the indexed diffraction patterns of fluorite samples, obtained using Origin 2017 software. The results show that all the XRD patterns of the ten (10) samples matched perfectly with that of the ICSD reference database. X' High Score Plus software calculated the unit cell parameters of the ten samples.

Table 2: The cell parameters, cell volume and density of the samples

Sample	a,b,c (Å)	Cell Volume (Å ³)	Calculated density (g/cm ³)
A	5.4528	162.12	3.20
B	5.4502	161.90	3.20
C	5.4502	161.90	3.20
D	5.4638	163.11	3.18
E	5.4630	163.04	3.18
F	5.4630	163.04	3.18
G	5.4626	163.00	3.18
H	5.4634	163.08	3.18
I	5.4530	162.15	3.18
J	5.4620	162.95	4.07

All the samples of natural fluorite belong to the cubic crystal system and space group of Fm-3m with Space group number 225, as expected. The interaxial angles are equal ($\alpha = \beta = \gamma = 90^\circ$) as for all cubic lattice structures. However, their values were slightly different regarding

the lattice parameters (Table 2). This is also presented in figure 5

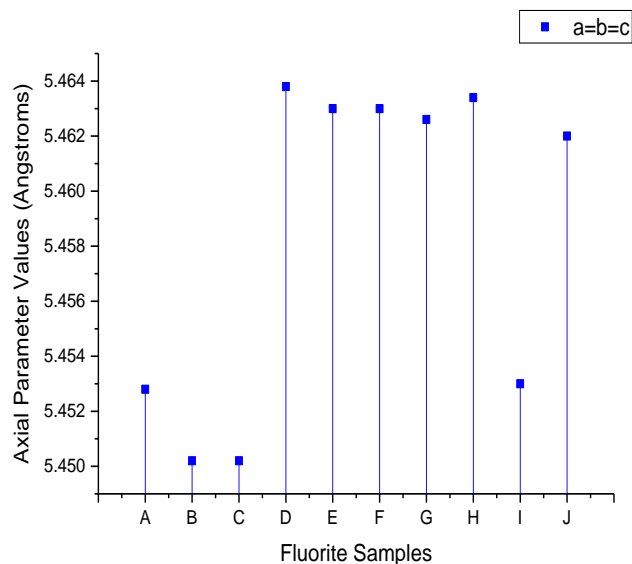


Figure 6: Axial Parameters of Natural Fluorite Samples

The samples' axial parameters and cell volume were slightly lower than that of the standard card ($a = 5.4631 \text{ \AA}$, $V = 163.0 \text{ \AA}^3$). This is because, in the formation of fluorite, some small-radius impurity elements (transition metals, rare earth elements and REEs) replace the original calcium element (*Ge et al.*,

2022). The closest axial parameter to the standard theoretical value was 5.4630\AA (in samples E and F). Based on this value, the unit cell structure of CaF_2 was constructed using the VESTA-win 64 software. The obtained structure shows a face-centered cubic lattice as the fluorite mineral unit cell structure (Figure 7).

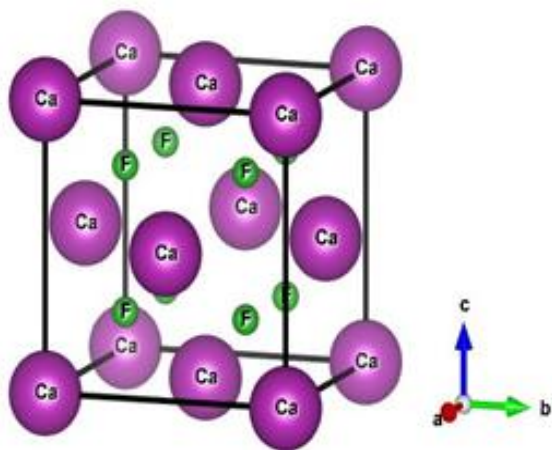


Figure 7: Unit cell structure of CaF_2

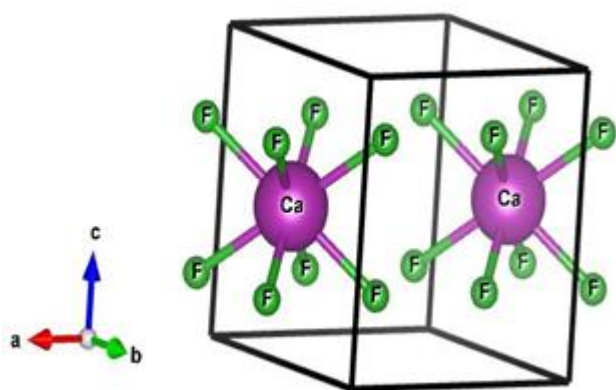


Figure 8: Calcium-Fluorine Coordination in CaF_2 unit cell structure

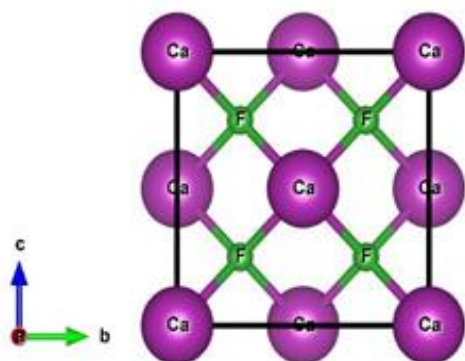


Figure 9: Fluorine-Calcium coordination in CaF_2 unit cell structure

The Ca-F ionic bond coordination has been illustrated in Figure 8 & 9. Each fluorine ion is surrounded by

four Ca ions and each is coordinated by eight F ions, arranged at the corners of a regular tetrahedron. This is consistent with the theoretical structural description of fluorite, meaning that the impurities found in the sample fluorite did not affect its ionic structure.

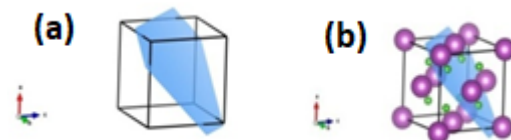


Figure 10 (a) & (b): (111) lattice planes in CaF_2 unit cell structure

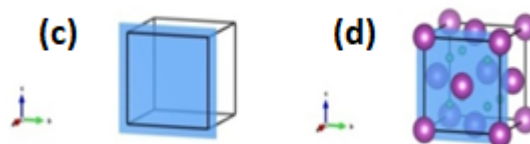


Figure 10 (c)&(d): (200) lattice planes in CaF_2 unit cell structure

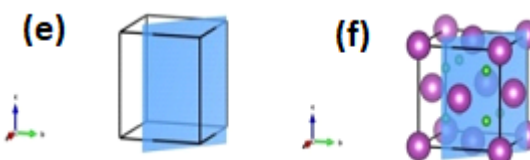


Figure 10 (e)&(f): (220) lattice planes in CaF_2 unit cell structure

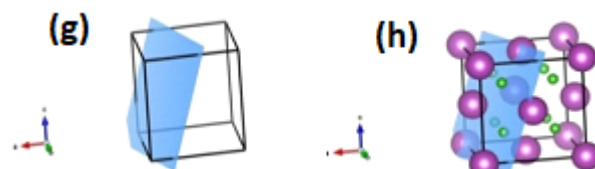


Figure 10 (g)&(h): (311) lattice planes in CaF_2 unit cell structure

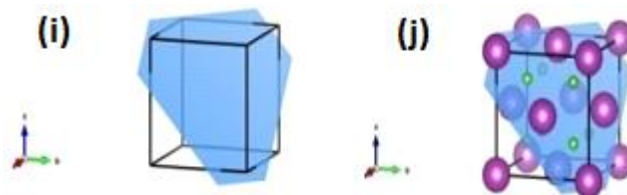


Figure 10 (i)&(j): (222) lattice planes in CaF_2 unit cell structure

The Miller indices were obtained from the simulated XRD pattern. The crystal (lattice) planes can be seen in Figure 10 (a) through (j). All planes are consistent with the theoretical geometric dimensions.

UV-Vis Spectrometry Results

Impurity elements make fluorite show different colours (Bill et al., 1978; Mitra S., 1981).

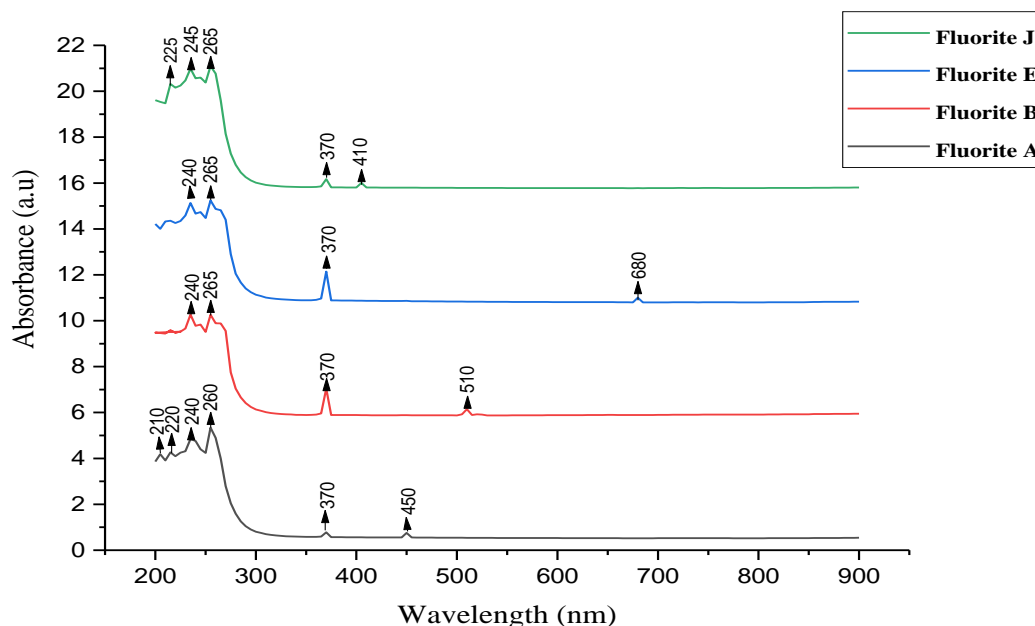


Figure 11 : UV-Vis Spectra for different fluorite samples

Figure 11 shows the UV-visible spectra of the four different coloured samples, Fluorites A, B, E and J. These samples were selected due to their different distinct colours. Fluorite A is bluish-green, Fluorite B is green, Fluorite E is black with some red at one edge and Fluorite J is black and partially light-purple in appearance. The remaining six samples, however, were replications of some of these four in colour. With the deepening of research, the formation of each colour seems to be due to more than one reason (Bill, 1982; Scouler, 1960). All the samples have absorption peaks between 209 to 368 nm, due to the absorption peaks of a certain impurity ion crystal field or a certain charge transfer peak. However, but these absorption peaks

may not affect the fluorite colour (Ge et al., 2022). The absorption bands close to 224 nm are caused by the electrons trapped in the Ca^{2+} interstitial, and those close to the 365 nm absorption band are caused by the holes trapped in the Ca^{2+} vacancy (Kim et al., 2013; Wenjun, 1999). The absorption peaks around 365 nm may be related to Ce^{3+} (Mitra, 1981). The absorbance in the visible range corresponds to their different colours showing consistency with the samples' colours.

Infrared Spectrometry Results

The infrared spectra of the four samples of natural fluorite are shown in Figure 12.

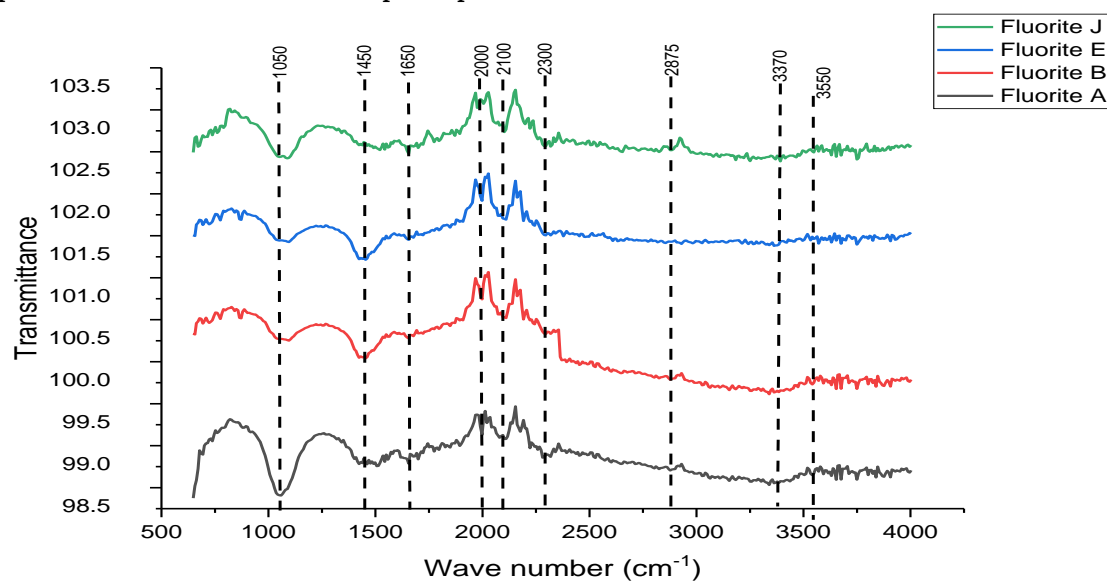


Figure 12: FTIR Spectra for different fluorite samples

The characteristic absorption peak of CaF₂ has a broad absorption band near 1050 cm⁻¹ in all the samples. This is consistent with the characteristic peak of fluorite at 1080 and 1110 cm⁻¹ recorded in the mineral spectroscopy (Zongming, 1990; Ge *et al.*, 2022). The absorption peaks at 1450 and 1650 cm⁻¹ are caused by CO₃²⁻ stretching vibration due to the CaCO₃ content (Ge *et al.*, 2022; Garrido-Cordero *et al.*, 2020; Jia *et al.*, 2019; Li *et al.*, 2017). The generation of 2000, 2100 and 2300 cm⁻¹ may be caused by CO₂ in the fluorite samples (Ge *et al.*, 2022; Megasari *et al.*, 2018). The absorption peaks at 2875 cm⁻¹ are due to the adsorption of oleic acid ester on the surface of fluorite is caused by the organic groups (Zhifeng *et al.*, 2015). The characteristic absorption peak at 3370 cm⁻¹ may be due to OH stretching vibration, indicating the existence of constitutional water in fluorite. The same phenomenon also exists in fluorite from China, India and Mexico (Ge *et al.*, 2022; Singh, 2013; Baatarsogt *et al.*, 2007).

CONCLUSION

Samples of natural fluorite from ten different locations were analyzed using X-Ray Fluorescence (XFR), X-Ray Diffraction (XRD) techniques, FTIR and UV-Visible spectrometry were used to find other mineralogical properties. XRF analysis determined the elemental composition of the sample. Calcium (Ca) has the most significant concentration. Fluorine was not detected in samples A due to the occurrence of its substitute Bromine (Br) and higher concentration of Ca. The concentration trace elements in the fluorite samples indicates calcium fluorite CaF₂. The structural configuration, lattice parameters and lattice planes confirmed a cubic structure. The fluorite samples were shown to have water content. Impurities in the fluorite samples were shown to affect their different colours.

ACKNOWLEDGEMENT

We acknowledge the efforts of Dr. Ahmed Rufa'i Usman, the Head of Physics Department, Umaru Musa Yar'adua, University, Katsina, for his support to see the success of this work.

REFERENCES

Altay., M., (2020). Thermoluminescence properties of two natural colorful fluorite samples of Anatolian origin for dosimetric applications. *Nuclear Inst. and Methods in Physics Research B*, 467, 33–39

- Akhter N, Mumtaz M, Hussain SS (2018). Quantification of Metallurgical Flux by Wavelength Dispersive X-Ray Fluorescence. *ChemSci J* 9: 195. [Crossref]
- Baatarsogt, B., Wagner T., Taubald H., Mierdel K., Markl G. (2007). Hydrogen isotope determination of fluid inclusion water from hydrothermal fluorite: Constraining the effect of the extraction technique. *Chem. Geol.*, 244, 474–482.
- Balaram, V. & Sawant, S.S (2022). Indicator Minerals, Pathfinder Elements, and Portable Analytical Instruments in Mineral Exploration Studies. *Minerals* 12, 394. [Crossref]
- Balogun F. A., Tubosun L A., Akanle A. O., Ojo J. O., Adesanmi C. A., Ajao J. A., & Spyrou I N. M (1996). INAA in the determination of the elemental constituents of a natural fluorite. *Journal of Radioanalytical and Nuclear Chemistry*, Vol. 222, Nos 1-2, 3538
- Balogun F.A., Ojo J.O., Ogundare F.O., Fasasi M.K. & Hussein L.A., (1999). TL response of a natural fluorite. *Radiat. Meas.*, [Crossref].
- Bill H., Calas G. (1978) Colour centers, associated rare-earth ions and the origin of coloration in natural fluorites. *Phys. Chem. Miner.* 3, 117–131.
- Bill H. (1982). Origin of the coloration of yellow fluorites: The O³⁻ center structure and dynamical aspects. *J. Chem. Phys.*, 76, 219–224.
- Dantas N.O., Chubaci J.F.D., & Watanabe S. (1998). Optical absorption bands and thermoluminescence peaks in heavily irradiated fluorites. *Radiat. Phys. Chem.* [Crossref].
- Dill, H.G (2016). Chemical, isotopic and mineralogical characteristics of volcanogenic epithermal fluorite deposits on the Permo-Mesozoic foreland of the Andean volcanic arc in Patagonia (Argentina). *Chemieder Erde (Geochemistry)* 76, 275-297
- Fawcett, T. G., Kabekkodu, S. N., Blanton, J. R., and Blanton, T. N. (2017). Chemical analysis by diffraction: the powder diffraction file. *Powder Diffr.* 32, 63–71.
- Garrido-Cordero, J.A.; Odriozola, C.P.; Sousa, A.C.; Gonçalves, V.S.(2020). Fluorite and

- translucent beads in Iberian Late Prehistory. *Mater. Manuf. Processes*, 35, 1424–1430
- Gates-Rector S., Blanton T. (2019). The Powder Diffraction File: a quality materials characterization database: International Centre for Diffraction Data, 12 *Campus Blvd, Newtown Square, Pennsylvania 19073-3273, USA*
- Ge X., Guo Q., Wang Q., Li, T., Liao L. (2022). Mineralogical Characteristics and Luminescent Properties of Natural Fluorite with Three Different Colors. *Materials*, 15, 1983. [[Crossref](#)]
- <http://nigeria.places-in-the-world.com/9411136-region2-ruwan-godiya.html>
- <http://commons.m.wikimedia.org/wiki/File:Fluorite-unit-cell-3D.png>
- Jenkins, R., Holomany, M., and Wong-Ng, W. (1987). On the need for users of the powder diffraction file to update regularly. *Powder Diffr.* 2, 84–87.
- Jia, C.P.; Qiao, C.H.; Wei, J.C.; Wang, H.M.; Shi, L.Q.; Ning, F.Z.; Liu, S.L.; Yang, M.Y.; Xu, X.; Dong, F.Y. (2019). The Study on the Mechanism of Fluorine Transformation between Water and Rock (Soil) in Seawater Intrusion Areas Based on FTIR Spectrum: *Spectrosc. Spectr. Anal.*, 39, 1036–1040.
- Jozanikohan G., Sahabi F., Hossain G. N., Memarian H. and Moshiri B. (2016). Quantitative analysis of the clay minerals in the Shurijeh reservoir Formation using combined X-ray analytical techniques. *Tebran, Iran* [[Crossref](#)]
- Kaduk J.A., Billinge S.J.L., Dinnebier R.E., Henderson N., Madsen I., Černý R., Leoni M., Lutterotti L., Thakral S. & Chateigner D. (2021). *Powder diffraction. Nat. Rev. Methods Primers*.1:77. [[Crossref](#)]
- Kim M., Yoon Y., Kang M., Shin D. (2013). Spectroscopic characteristics of natural fluorite induced by electron-beam irradiation: *J. Ceram. Processing Res.*, 13, 541–546.
- König, U., (2021). Nickel Laterites—Mineralogical Monitoring for Grade Definition and Process Optimization. *Academic Editor: Fang Xia* [[Crossref](#)]
- Mao M., Simandl G.J., Spence J. and Marshall D., (2015). Fluorite trace-element chemistry and its potential as an indicator mineral: Evaluation of LA-ICP-MS method. In: Simandl, G.J. and Neetz, M., (Eds.), *Symposium on Strategic and Critical Materials Proceedings*, Victoria, British Columbia. British Columbia Ministry of Energy and Mines, British Columbia. *Geological Survey Paper* 2015-3, pp. 251-264.
- Megasari, E.; Dharsono, H.D.; Fadil, R.; Zakaria, M.N.; Widyaputra, S.S.; Cahyanto, A. (2018). The Evaluation of Setting Time and FTIR Spectroscopy of Carbonate Apatite Cement as Endodontic Sealer. *Key Eng. Mater.* 782, 32–37
- Mitra S. (1981). Nature and genesis of color centres in yellow and colorless fluorite from Ambadongar, Gujarat, India. *Neues Jahrb. Mineral.* 141, 290–308.
- Öztürk, H (2019). Rare Earth Element-bearing Fluorite Deposits of Turkey: an overview
- Polymeris G.S., Kitis G. & Tsirliganis N.C (2006). Correlation between TL and OSL properties of CaF₂:N. *Nucl. Instrum. Meth. Phys. Res. Sect. B* 251,133–142, [[Crossref](#)].
- Scouler, W.J. (1960). Effect of Mono- and Trivalent Cations on Color Centers in Calcium Fluoride. Technical Report 147; Massachusetts Institute of Technology. *Laboratory for Insulation Research*: Cambridge, MA, USA.
- Singh R.K. (2013). FTIR spectroscopy of natural fluorite from Ambadongar, Gujarat. *J. Geol. Soc. India*, 81, 215–218.
- Smaalen, S.(2013). *Modern Diffraction Methods*. Boschstr. 12, 69469 Weinheim, Germany: *Wiley-VCH Verlag GmbH & Co. KGaA*
- Wenjun L. (1999). Restudy of black fluorite in the Huayuan lead-zinc deposit. *Chengdu Li. J. Eng. Coll.*, 26, 101–105.
- Zhifeng Y., Hong X. (2015). Study on the evolution characteristics of metallogenic fluid in Yaogangxian tungsten deposit: *Human Province. Miner. Depos.* 4, 309–320.
- Zongming W. (1990). *Practical Infrared Spectroscopy*, 2nd ed.; *Petroleum Industry Press: Beijing, China*.